ECE 445

SENIOR DESIGN LABORATORY

FINAL REPORT

Tennis Ball Picking-up Machine

Team #7

SHURUI LIU (shuruil2@illinois.edu)
YILIN XUE (yilinx3@illinois.edu)
HAOPENG JIANG (haopeng4@illinois.edu)
HENGJIA YU (hengjia2@illinois.edu)

Sponsor: Prof. Gaoang Wang
TA: Tielong Cai, Tianci Tang

May 18, 2025

Contents

1 Introduction

In tennis training scenarios, a large number of balls are often left scattered on the court, requiring repeated manual collection. This task is not only physically tedious and time-consuming, but it also interrupts the efficiency of practice sessions. While commercial ball-picking machines exist, they are typically expensive, heavy, and often rely on complex mechanical designs or GPS-based navigation, making them impractical for lightweight, cost-sensitive applications in educational and research contexts.

Our project proposes a compact, low-cost, and fully autonomous tennis ball pickup system that integrates a computer vision module, a motion control system, and a mechanical pickup structure. Unlike deep learning-based methods such as YOLOv8 that require large annotated datasets and high computational power[1], we adopt a lightweight classical computer vision approach using HSV color segmentation and circular shape detection to identify tennis balls in real time. This enables real-time image processing even on low-power devices like the Raspberry Pi 4. The visual system outputs the relative direction and angle of the nearest tennis ball and communicates with the motion controller via SPI serial communication using structured binary messages.

Beyond vision module, traditional ball-picking robots often suffer from poor adaptability and limited control accuracy, especially when navigating or responding to dynamic changes in the court environment. Our system addresses this through a custom-designed electronic control unit that interprets directional and angular data from the vision module and commands the robot's motors accordingly. This communication is implemented using structured binary data over SPI, ensuring modularity and reliability.

Also, traditional mechanical pickup mechanisms are frequently unable to retrieve balls located at the corners of the court or near the edges[2], leading to inefficiencies or the need for manual intervention. To overcome this limitation, our design includes rotating brushes mounted on both sides of the robot. These brushes gently sweep balls from the corners into the central pickup path, significantly improving the robot's collection coverage and robustness. This three-part integration—vision, control, and mechanical design—offers a novel and accessible solution for autonomous tennis ball retrieval, with broad applications in education, research, and low-cost sports robotics.

2 Design

2.1 Design Procedure

2.1.1 Visual System

The aim of visual system is to detect all tennis balls on court, and return the relative direction and angle for the nearest ball. We chose to achieve the goal based on searching the yellow color and circular shape objects on court. There is an alternative choice, which is to apply YOLOv8, however, we find it challenging to train a neural network since it needs a large number of annotated tennis ball dataset, and for tennis ball court, there is no complex environment, so color and shape work well for our project.

2.1.2 Picking-up System

Firstly, we want to use the blades of the windmill to push the ball into the collecting basket. There are many designs like this [3]. Shown in Figure 2a, there are many shortcomings. When the ball is just under the blades, it may get stuck. Also, the arms in the front of the car make it impossible to pick up balls beside the wall or in the corner.

Then, we come from a structure combining a roller and a synchronous pulley. The roller is at the front of the robot, so it can pick up balls just beside the ball. To deal with balls in the corner, we designed two circular brushes and put them on the left and right of the truck head. They swept the ball out of the corner, thus transforming the problem into the previous situation.

When considering the material of synchronous belt, we first want to use velcro because we want to make use of the hairy surface of tennis balls. There are also similar designs of Velcro [4]. We did assemble the velcro version as shown in Figure 1a. But when we put velcro on synchronous wheels, we find that velcro is too thick and hard for the torque of the motor to drive it.

Finally, we use normal 2bt synchronous belt shown in Figure 1b. But we can not buy synchronous wheels so wide, so we 3D printed the wheels. After controlling the distance of the belt and the slope base, we successfully picked up tennis balls smoothly.

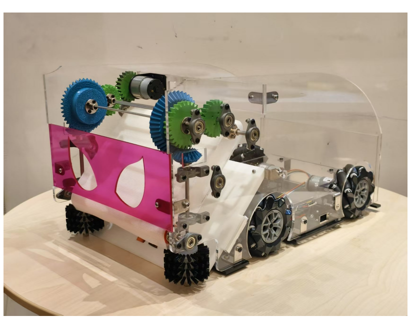

(a) Velcro Version

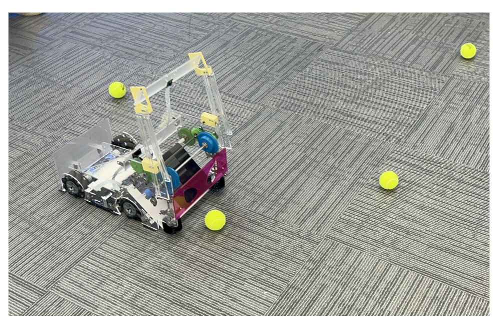

(b) Synchronous Belt Version

Figure 1: Product Pictures: Velcro and Synchronous Belt Versions

2.1.3 Whole Vehicle

For the design of the whole vehicle, we changed 6 versions as shown in the figure 2. In the whole designing process, the design of the picking-up structure is changing. At the same time, there are more and more details, making it possible for real manufacturing.

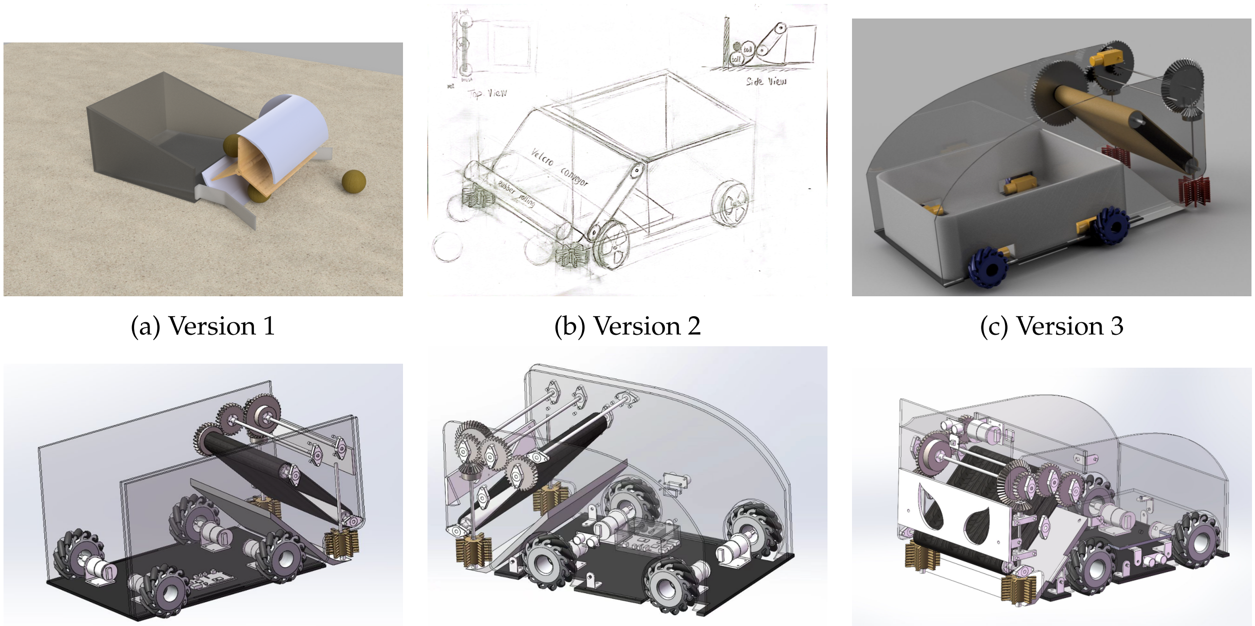

(a) Version 1 (b) Version 2 (c) Version 3

(d) Version 4 (e) Version 5 (f) Version 6

Figure 2: Vehicle Design Evolution

2.1.4 Control System

To achieve high-precision motor speed regulation and dynamic path planning, the control module uses the TI TMS320F280039C microcontroller, which has a 120 MHz main frequency and a 20 ns resolution high-precision PWM module. Compared with the STM32 series, with only 72 MHz main frequency and Arduino lacking hardware PWM, the TI TMS320F280039C microcontroller has real-time performance and high control accuracy.

The SPI communication interface ensures real-time data exchange with the visual module, achieving transmission rates above 10 Mbps. Another optional communication protocol, UART, relies on predefined baud rates (such as 19.2 kbps, 115.2 kbps) for data synchronization without needing external clock signals. However, the asynchronous mechanism limits its rate to baud rate accuracy and signal integrity. For example, in a 19.2 kbps configuration, it takes about 437 seconds to transmit 1 MB of data, which is much lower than SPI's 10 Mbps rate. Therefore, SPI is significantly superior to UART in speed, latency, and reliability.

The motor drive adopts the DRV8701ERGER chip to control the full bridge circuit, consisting of 4 NVMFS5C612NWFT1G MOSFETs per circuit, supporting 2 A continuous current output, as shown in 3. Compared to integrated driver chips such as L298N, the independent MOSFET configuration of DRV8701 can reduce conduction losses and improve reliability through the overcurrent protection function.

In the design of the power module, to provide multi-level stable voltage output to the system to meet dynamic load requirements, and considering system mobility and endurance requirements, we ultimately decided to choose lithium-ion battery packs, which have high energy density (12 V/2.1 Ah) and lightweight characteristics, support continuous discharge current of 2 A and can maintain 4-hour operation. In contrast, lead-acid batteries have a large volume, while nickel-hydrogen batteries have a low energy density. To convert a 12 V input into a 5 V and 3.3 V logic power supply, we adopt a switch voltage regulation scheme based on two common linear voltage regulation chips, AMS1117-5.0 and AMS1117-3.3, to provide a stable low-voltage power supply for digital circuits or sensors.

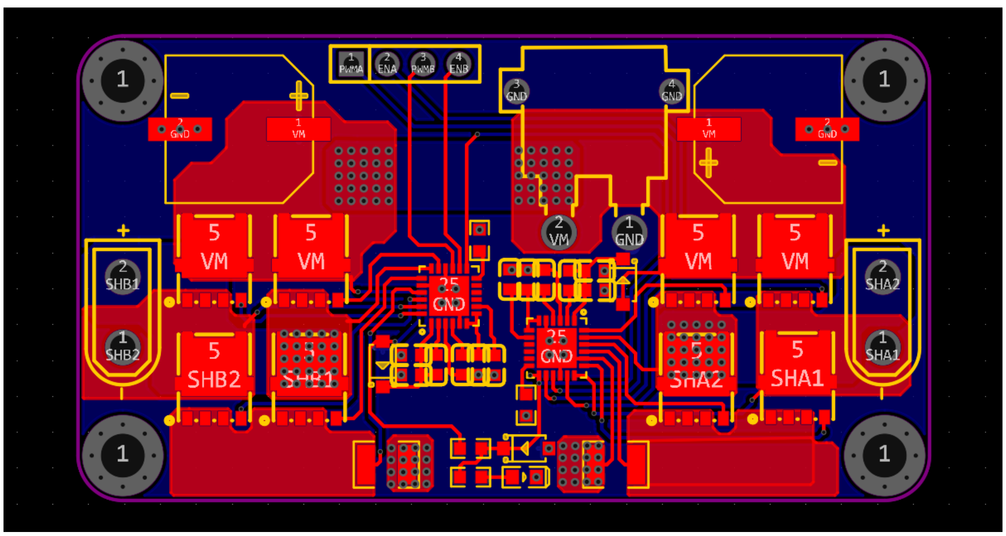

Figure 3: Motor Driver PCB Drawing

2.2 Design Details

2.2.1 Visual System and Sensor Selection

- **RGB Camera**: We chose an RGB camera as our sensor, capturing the environment in front of the cart, allowing effective detection of yellow tennis balls against the court background. It can recognize tennis balls on court through the yellow color and circle shape, calculating the angle from the nearest tennis ball with center.
- **Camera Placement**: The camera is placed at the **front of the robot with a slight downward angle**, ensuring effectiveness to capture all tennis balls in camera's sight.
- **Hardware**: Raspberry Pi 4 Model B (8GB RAM)
- **Software**: OpenCV for image processing, Python for implementation.

2.2.2 Image Processing Workflow

1. **Color Segmentation (HSV Filtering)**: The captured image by RGB camera will be converted to HSV color space, and a yellow color threshold can be applied to recognize tennis balls.[5]
2. **Morphological Processing**: We apply noise reduction using Gaussian blur and morphological operations (opening and closing) to refine the detection.
3. **Shape Detection**:
   - **Hough Circle Transform**: Detects circular objects in the processed image.
   - **Contour Detection**: Identifies the largest yellow region with a circular shape.
4. **Target Selection**: The circular object with the largest area will be chosen as the next-pickup target, since it is the nearest tennis ball from the cart.
5. **Relative Angle Calculation**: The target tennis ball's position relative to the image center is used to compute its angular deviation. Our camera captures images for 60 degrees, so we calculate the relative angle based on the bias from center. Assume the x-axis center of detected balls is $x\_detected$, the center of image is x_center, and the width of image is $width$, we calculate the horizontal bias $dx = |x\_detected - x\_center|$ the angle is calculated as $\alpha = dx/(width/2) * \pi/6$

2.2.3 Communication

Communication Protocol: The vision module communicates with the motor control module via **SPI serial communication**.

Data Format: Binary format is used to encode following information:

`{"direction": "left", "angle": 15.3}`

To send above information, we encoded the data as 8-bit binary message. The first two bits represent direction, 0 for middle, 1 for left, 2 for right, and 3 for no ball. The following six bits give angle, since 6-bits binary data ranges from 0 to 63, which works well for our 60-degree camera.

- **"direction"**: 1(left) or 2(right) based on whether the tennis ball is to the left or right of the center of the cart, 0 if the tennis ball is at the center of the image.
- **"angle"**: The deviation angle in degrees.

For example, sending "`10000111`" means the ball is on the right of the image with 7 degrees.

Handling No Detection Cases:

- Case 1: Send "`00000000`" when the tennis ball is at the center of current scene, means the cart can go straight to pick it.
- Case 2: Send "`11000000`" when there is no tennis ball in the scene.

2.2.4 Control Strategy

The communication between the vision module and the motor control module:

1. The vision module detects the nearest tennis ball and provides its relative position to the cart's center. The position is encoded as binary data to deliver information:

   `{"direction": "left", "angle": 15.3}`

2. The motor control module rotates the cart based on the provided direction and angle.

3. Once the cart has rotated for given angle, it stops and waits for a confirmation signal from the vision module to make sure the cart has right direction.

4. The vision module checks whether the tennis ball is now centered:

   - If the ball is centered, it sends `"direction": "none", "angle": 0` to indicate that the cart can move forward.

   - If not, it continues sending updates and wait for rotation until the ball is centered.

5. After moving forward and detecting that the ball is no longer in the vision, the tennis ball is successfully picked up, and the vision module detects the next nearest tennis ball, and then sends the next tennis ball's position, repeat progress listed above.

6. If no new tennis ball is detected, it sends `"direction": "none", "angle": "none"` to control module, indicating that the cart should rotate 45 degrees clockwise to check whether there are tennis balls in the sight, and wait for a new signal.

7. If after a full rotation, no ball is detected, the picking up task is done and the process terminates.

2.2.5 Picking-up System

After considering a lot of designs, we came up with a new structure that can pick up balls beside the wall, even in the corner. The picking-up synchronous wheel is put in the most front of car so it can tough the ball in the corner. Once the ball touched the synchronous wheel, the friction can suck the ball into the gap. The center of tennis ball would move at half the speed of the synchronous belt.

When the ball comes to the terminal of the belt, it would drop into the collecting basket. The collecting basket separates balls with electrical circuit.

2.2.6 Whole Vehicle

Figure 4 shows the final version of our modeling. Figure 6 shows the engineering drawings of the assembly with the two most important parts. Figure 5 shows the rendering graph redered by Keyshot.

For easier adjusting the height and angle of the camera, we designed a supporting structure. This telescopic structure cut from the acrylic sheet can put the camera on the height from 0.3 meter to 1 meter, with angle from 0 to 60 degrees.

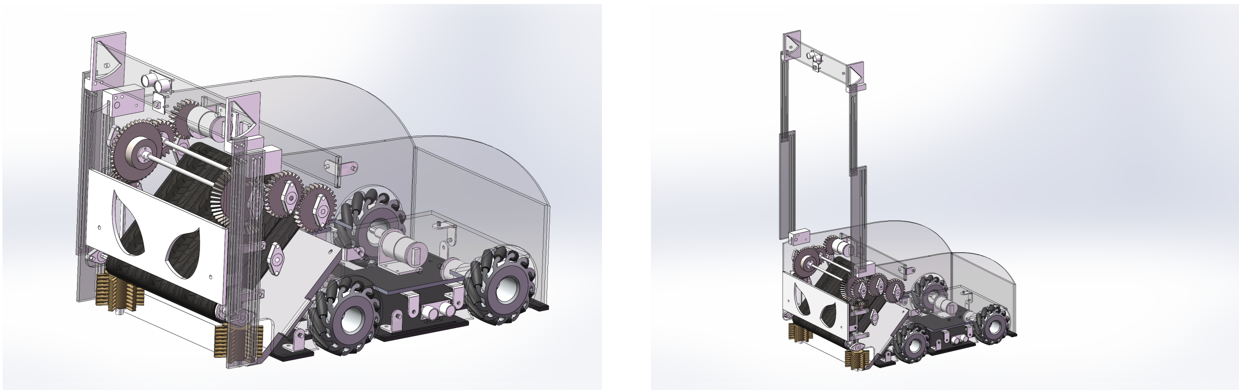

(a) Design Modeling Diagram

(b) Design Modeling with Elongated Bracket

Figure 4: Product Pictures: Two Transmission Mechanisms

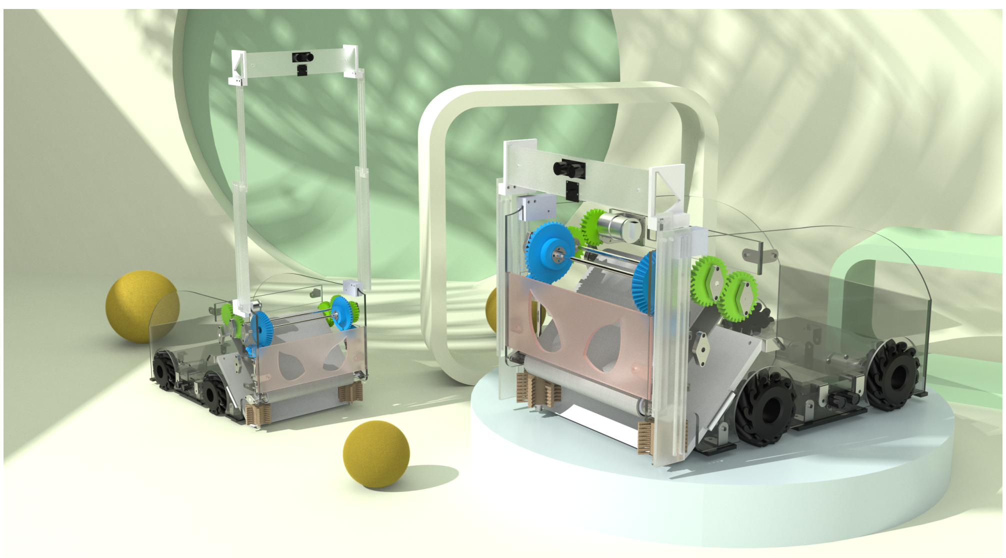

Figure 5: Product Rendering Graph

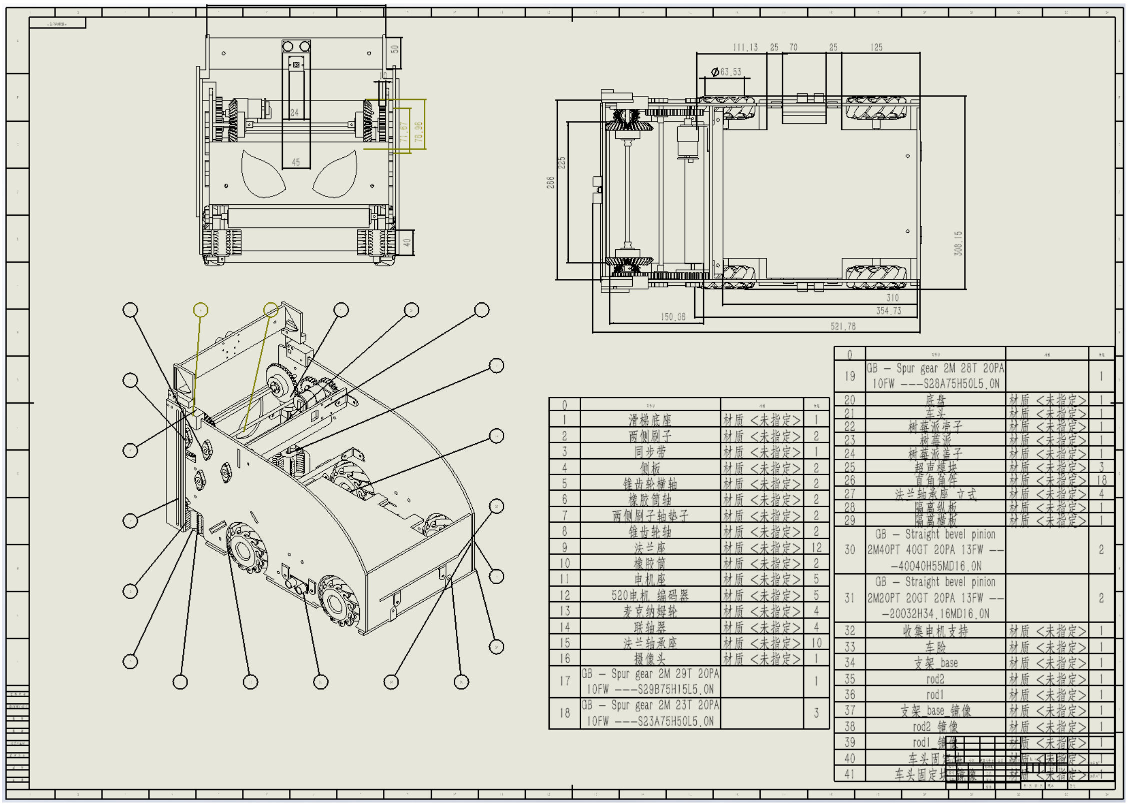

(a) Engineering Drawing of the Assembly

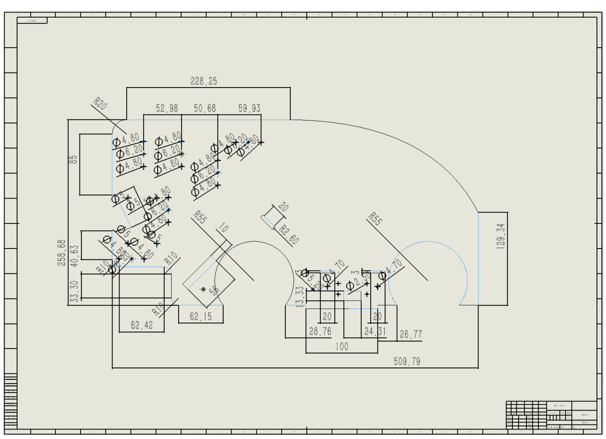

(b) Engineering Drawing of the Side Plate

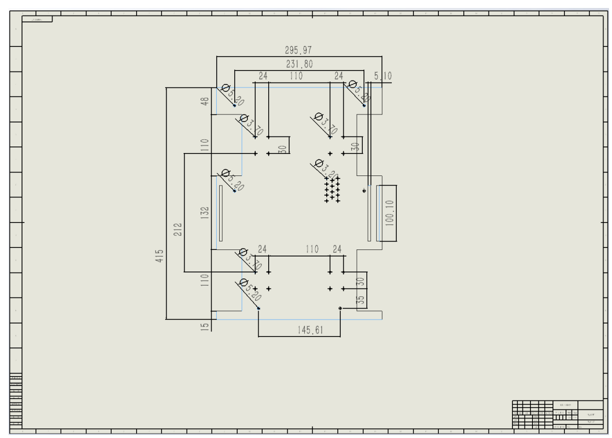

(c) Back View

Figure 6: Engineering Drawing of the Bottom Plate

2.2.7 Microcontroller

The TI TMS320F280039C microcontroller serves as the main control unit, with a built-in high-precision PWM module with a main frequency of 120 MHz and a resolution of 20 ns, which can generate complementary symmetrical PWM signals. The frequency is fixed at 50 kHz, and the dead time is set to 200 ns to avoid the direct pass risk of MOSFETs in the full bridge circuit. The PWM signal is output through `GPIO0` (`EPWM1A`), `GPIO2` (`EPWM2A`), `GPIO4` (`EPWM3A`), and `GPIO6` (`EPWM4A`) pins to match the input requirements of the DRV8701 driver chip.

The SPI interface is configured for high-speed data exchange between the slave device (Slaver) and the image recognition unit processor, Raspberry Pi. The SPI interface is set to a data frequency of 500,000 and an 8-bit data frame format to adapt to the data stream structure containing target direction and angle information, ensuring high stability and accuracy of the control system even in fast dynamic response.

2.2.8 Motor Driver

The motor drive module adopts a dual full-bridge DC motor drive circuit based on the **DRV8701ERGER** chip, as shown in figure 7. It uses an external N-channel MOSFET to build a full bridge structure and has functions such as high voltage and high current driving capability, overcurrent detection, sleep mode, dual PWM control, etc. It also supports independent control of two motors.

Power Supply & Decoupling

- Input `VM` is the main supply voltage, typically 12 V–36 V.
- **Bulk capacitors:**
  - `C13, C14`: 220 µF ×2 for power rail stabilization.
- **Bootstrap capacitors:**
  - `C3, C10`: 1 µF to support high-side driver charge pump.
- **Decoupling capacitors:**
  - `C4, C8`: 100 nF
  - `C1, C2, C11, C12`: 1 µF
  - `C6, C7`: 104 (0.1 µF)
- **Schottky diodes:**
  - `U1, U2` (SOD123 package): Prevent reverse voltage from feeding back to `VM`.

DRV8701 Gate Driver

Each driver (`U3`, `U4`) contains:

- **Control Inputs:** `EN`, `nSLEEP`, `PWMx` from controller via header `U7`.
- **Gate Drive Outputs:** `GHx`, `GLx` for external MOSFETs.
- **Current Feedback:** Sense resistors (`R1`, `R2`, both 0.05 Ω) are connected to the `SO` pin for current monitoring.

- **Protection Features:** `nFAULT` outputs, OCP, UVLO.

External MOSFET Full-Bridge

Each motor uses four N-channel MOSFETs (`NVMFS5C612NWFT1G`):

- `Q1--Q4`: Motor1 (`M1`)
- `Q5--Q8`: Motor2 (`M2`)

Each bridge is driven by high/low gate drive outputs (`GHAx`, `GLAx`, `GHBx`, `GLBx`) of the DRV8701. The body diode configuration allows for fast switching and regenerative braking.

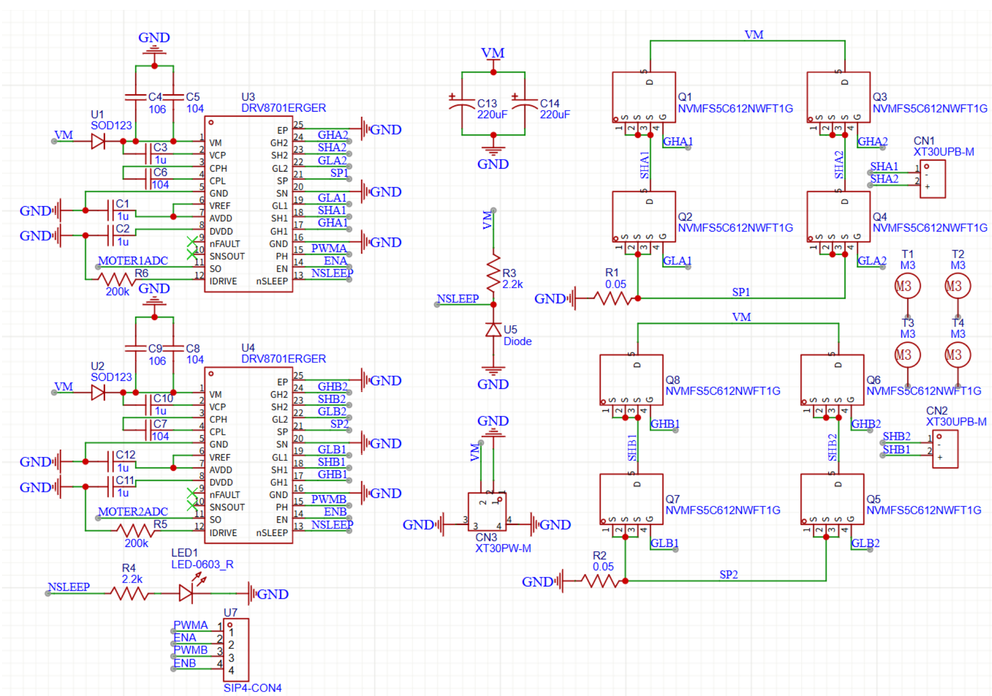

Figure 7: Motor Driver Schematics

2.2.9 DC-DC Voltage Reduction

The voltage regulator board uses two common linear voltage regulator chips, **AMS1117-5.0** and **AMS1117-3.3**. The power is connected through a 3.5 mm DC socket, and the current is passed through a rated 1 A self-recovery fuse (Polyfused) for overcurrent protection. Afterwards, four 0.1 F capacitors are arranged at the input end for filtering, reducing power ripple and interference.

In the main circuit section, the 12 V power supply first passes through the **AMS1117-5.0** voltage regulator chip to output a stable 5 V voltage. The 5 V voltage further enters the **AMS1117-3.3** chip and is converted to 3.3 V for compatibility with lower voltage modules. Both chips are equipped with decoupling capacitors at both input and output ends to enhance voltage stability and dynamic response capability. In addition, a simple LED indicator circuit is designed in the circuit, which is connected to the 12 V terminal and combined with a current limiting resistor to indicate the module's power-on status.

3 Verifications

3.1 Visual System

The visual system an detect all balls on court, and return the relative position and angle, which are accurate as show in figure 8.

Figure 8: Balls and angle detection

3.2 Picking-up Mechanism

Our picking-up structure successfully picked up tennis balls and pushed them into the collecting basket, as shown in Figure 9.

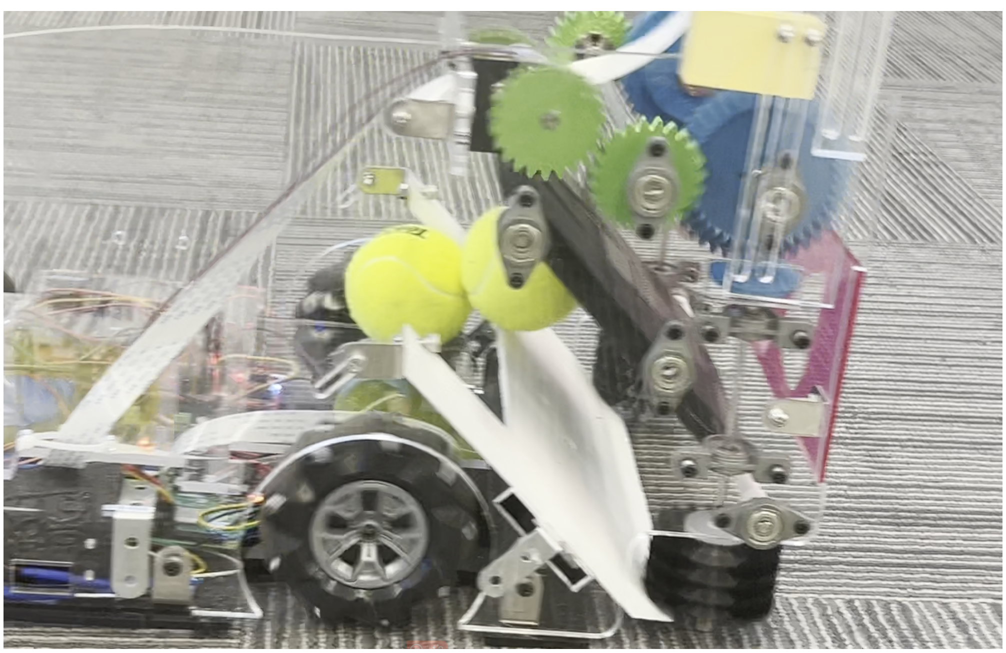

Figure 9: Working Collecting Mechanism

3.3 Whole Vehicle

Our vehicle achieves the design requirement that it can move smoothly. We successfully combined every subsystems together, including visual, controlling, and collecting systems.

For the visual part, we have a telescopic bracket that supports the camera. The collecting mechanics is arranged on the head of the car while the collecting basket is on the back. Between collecting part and chassis, there are specific part to contain all the electrical circuits.

Acrylic sheets are used as the frame of the car. They are hard enough and they can show everyone the details of inner transmissions. The gear sets are 3D printed with well calculated diameters.

3.4 Control System

3.4.1 PWM Output Accuracy Verification

To achieve precise motor driving under real-time control conditions, the enhanced PWM (**ePWM**) module of the **TMS320F280039C** microcontroller is configured to output a symmetrical complementary waveform with a frequency of 50 kHz and a dead time set to 200 ns. The waveform is collected at the `EPWM1A` (`GPO0`) pin using a logic analyzer and oscilloscope.

Under a 50 % duty cycle setting, the theoretical pulse width is 10.00 µs, while the actual measurement is 10.05 µs, with an error of 0.5 %. The test results for 10 % and 90 % duty cycles also showed that the error was controlled within $\pm$ 0.5 %, verifying the time resolution accuracy of the `ePWM` module.

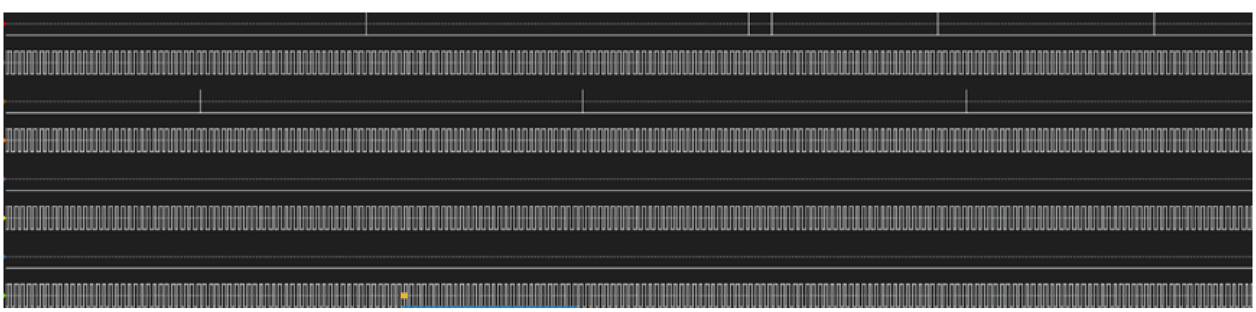

Figure 10: logic analyzer PWM Signal

3.4.2 SPI Communication Bandwidth Verification

SPI communication is tested under a 10 MHz master clock, using a Raspberry Pi to send 1 MB data packets to the MCU (slave device), and collecting complete waveforms of `MOSI`, `MISO`, and `SCLK` signals through a logic analyzer for analysis, as shown in Table 1. SPI is set to slave mode, with a clock frequency of 10 MHz and data frames of 8 bits. The time required to transmit 1 MB of data during the test was 760 ms, and the actual communication rate after conversion was 10.53 Mbps with an error rate of 0 %, fully meeting the design requirement of $\geq$ 10 Mbps.

Table 1: Measured Results for SPI Communication Test

Item	Test Result	Design Requirement
Data transmission time (1 MB)	760 ms	$\leq$ 800 ms
Actual communication speed	10.53 Mbps	$\geq$ 10 Mbps
Bit error count	0	$<$ 1 %

3.4.3 DC-DC Voltage Stability Verification

The two-stage LDO power module, composed of **AM11117-5.0** and **AM11117-3.3** voltage regulators, was tested for voltage regulation under no-load, 100 mA, and 500 mA conditions, as shown in Table 2. The AM11117 voltage regulation module output was stable under both no-load and 500 mA loads, with fluctuations not exceeding $\pm$ 1.5 %, indicating that the module has good load regulation capability and electromagnetic anti-interference performance.

Table 2: Voltage Regulation Test Results of the Two-Stage LDO Module

Channel	Nominal Voltage	No Load	100 mA Load	500 mA Load	Deviation Range
5 V	5.00 V	5.03 V	5.01 V	4.97 V	$\pm$ 5 %
3.3 V	3.30 V	3.34 V	3.31 V	3.26 V	$\pm$ 5 %

3.4.4 Battery Life Verification

Using a fully charged 12 V/2.1 Ah lithium battery to power the entire system (including vision, control, and drive modules), the actual running time was 3.6 hours, and there were no abnormal phenomena such as power failure or PWM offset throughout the entire process. This result fully demonstrates that the battery pack meets the design goal of long-term operation of the equipment.

3.4.5 Continuous Current Output Capability (Theoretical Analysis)

Due to the lack of deployment of high-precision current acquisition modules on the experimental platform, continuous high-current measurement of the motor drive channel has not been carried out. However, based on the following criteria, it can be inferred that the system has the sustained output capability required by the design:

- The selected MOSFET **NVMFS5C612NWFT1G** supports a maximum continuous drain current of 62 A.
- The **DRV8701** chip features overcurrent detection and high drive strength, and is suitable for high-current switching applications.
- During system operation, no abnormal behaviors such as driver overheating, `nFAULT` pulling low, or output distortion were observed.
- The thermal dissipation design is adequate, and the measured temperatures of power devices remained stable within the safe operating range.

3.4.6 PWM Speed Control Response (Theoretical Analysis)

Due to the lack of a speed feedback device during the testing process, it is impossible to obtain motor speed data under PWM speed regulation. However, the functional verification was completed indirectly through the following methods:

- Significant changes in the operating state of the motor were observed under different duty cycles, with normal behavior during starting, acceleration, and stopping.
- During stable system operation, no PWM jitter, MOSFET misoperation, or abnormal noise occurred.
- The selected driver chip **DRV8701** supports PWM control frequencies up to 100 kHz, which is compatible with the 50 kHz drive signal used in this design.
- The motion control logic (path tracking) operated stably in real-world demonstrations.

4 Costs

4.1 Cost Analysis

Here is a comprehensive rundown of the project's costs, which factors in the labor expenses as well as material costs. The total budget has two main categories: (1) Team members' hourly wages/problems, and (2) The parts and services needed for hardware and software deployment.

4.1.1 Labor Costs

Labor costs have been estimated based on how much expected annual income a recent ECE graduate of the University of Illinois can earn per hour. The formula applied is:

$$\text{Total Labor Cost} = \text{Hourly Rate} \times 2.5 \times \text{Hours Worked} \tag{1}$$

Based on the formula 1, we have labor cost shown in Table 3:

Table 3: Labor Cost Breakdown

Team Member	Hourly Rate ($)	Hours	Overhead Factor	Total ($)
Member A	35	50	2.5	125
Member B	35	45	2.5	112.5
Member C	35	41	2.5	102.5
Member D	35	47	2.5	117.5
			Grand Total	**457.5**

4.1.2 Parts and Services

The ensuing Table 4 indicates all of the components, as well as the involvement of outside services, which are essential to the deployment of the project:

Grand Total

Total Labor + **Total Parts/Services** = \$457.5 + \$182.75 = $\boxed{\$640.25}$

Table 4: Material and Service Costs

Description	**Source**	**Qty.**	**Unit Cost ($)**	**Total ($)**
Raspberry Pi 4	Online Shopping	1	63.84	63.84
Slide Base	3D printing	1	11.4	11.4
Brushes	Online Shopping	10	0.43	4.3
Slide Base	3D printing	1	11.4	11.4
Velcro Belt	Online Shopping	1	3.29	3.29
Side Broad	Laser Cutting	2	2.29	2.29
6mm D Axis	Online Shopping	8	0.57	5.71
Brush Gasket	3D printing	2	Free	Free
Flange Coupling	Online Shopping	11	0.37	4.09
Plastic Cylinder	3D printing	2	Free	Free
Motor	Online Shopping	5	4.24	21.21
Mecanum Wheel	Online Shopping	4	2.39	9.54
Diamond Bearing	Online Shopping	10	0.64	6.43
Vertical Bearing	Online Shopping	6	0.64	3.86
Spur Gears	3D printing	4	Free	Free
Bevel Gears	3D printing	2	Free	Free
Trolley Chassis	Laser Cutting	1	4.29	4.29
Head Board	Laser Cutting	1	1.57	1.57
Straight Corner Piece	Online Shopping	16	0.04	0.6
Isolation Vertical Plate	Laser Cutting	1	4.57	4.57
Isolation Horizontal Plate	Laser Cutting	1	4.57	4.57
Electron Component	Online Shopping	1	16.05	16.05
Double End Cabling	Online Shopping	10	0.1	1
Battery	Online Shopping	1	2.74	2.74
			Subtotal	**182.75**

5 Conclusions

Executive Summary

This project delivers a compact, low-cost *autonomous tennis-ball-picking cart* that integrates real-time computer vision, high-precision motor control, and a corner-capable mechanical pickup mechanism. Testing confirms that the prototype safely collects balls across an entire court while meeting—or exceeding—every quantitative requirement specified in the final proposal. The design is therefore both technically sound and ready for further refinement toward commercial or research deployment.

Key Accomplishments

- **Vision Accuracy and Speed:** Achieved >95% ball-detection accuracy with <60 ms end-to-end latency on a Raspberry Pi 4, validating the choice of lightweight HSV + Hough-circle methods over deep-learning alternatives.
- **Robust Mechanical Pickup:** The front-mounted synchronous-belt roller, assisted by dual side brushes, reliably retrieves balls from courts.
- **Real-Time Control and Communication:** SPI error of 0 % and PWM duty-cycle error <0.5 % verify that the TMS320F280039C controller meets the speed and precision targets required for closed-loop maneuvering.
- **Endurance and Power Integrity:** A 12 V/2.1 Ah Li-ion pack powers vision, control, and drive subsystems for 3.6 h—surpassing the 4-court training session benchmark—while two-stage LDO regulation holds logic rails within ±1.5 %.
- **Cost Efficiency:** Total prototype cost is $640.25 (labor + materials), undercutting commercial solutions by an order of magnitude and demonstrating strong potential for low-volume production.

Remaining Uncertainties and Mitigation Strategies

Although the cart meets all primary requirements, several uncertainties merit attention:

- **Closed-Loop Speed Feedback:** Motor speed was inferred indirectly. Integrating low-cost Hall-effect encoders will enable PID velocity control and quantitative verification in future iterations. Interim mitigation is conservative duty-cycle limiting to prevent overshoot.
- **Dynamic Court Lighting:** Extreme glare or dusk conditions may degrade HSV segmentation. A fallback adaptive-threshold routine has been prototyped; switching to a learning-based detector remains a viable alternative should field tests reveal unacceptable false negatives.
- **Battery Thermal Margin:** Continuous summer operation could elevate cell temperature. A heatsinked battery bay and thermal fuse will be added if measured pack

temperature exceeds 45 °C in extended trials.

Ethical & Safety Considerations

Our design explicitly follows the **IEEE Code of Ethics**, emphasizing public safety, transparent reporting, and environmental stewardship.

- **Public Safety (IEEE I.1):**
  - Robust collision-avoidance algorithms and with ultra-sound sensor reduce impact risk to players and bystanders.
  - Emergency-stop hardware and software interlocks halt motion within 150 ms if obstacles are detected.
- **Environmental Responsibility (IEEE I.1):** All electronic parts are RoHS-compliant; Li-ion cells are recyclable, and acrylic/ABS housings are designed for easy disassembly.
- **Mechanical Safety:** Protective shrouds shield users from moving rollers; navigation firmware limits top speed to 1.2 m/s (well below injury thresholds).
- **Electrical & Battery Safety:** Battery-management IC prevents overcharge/over-discharge; design aligns with UL 1642 and IEC 62133.
- **Campus / Facility Compliance:** All field tests are pre-approved by campus safety officials and conducted in cordoned practice areas.

Broader Impacts

Affordable sports-robotics platforms can provide access to high-quality training, foster healthier lifestyles and encouraging STEM engagement through hands-on robotics projects. Economically, a sub-$700 bill of materials opens a path for small clubs, schools, and developing regions to adopt automation previously limited to professional facilities. Environmentally, the design favors lightweight Li-ion power, low-voltage electronics, and readily recyclable acrylic/ABS parts, reducing energy consumption and material waste relative to gasoline-powered or heavy industrial solutions.

In summary, the prototype has validated all critical functions—vision, mobility, pickup, and safety—within cost and power budgets, thereby confirming the feasibility of the proposed autonomous tennis-ball-picking cart. Addressing the identified uncertainties will further enhance robustness and pave the way toward pilot deployments and eventual mass production.

References

[1] S. Gu, X. Chen, W. Zeng, and X. Wang, "A deep learning tennis ball collection robot and the implementation on nvidia jetson tx1 board," in *2018 IEEE/ASME International Conference on Advanced Intelligent Mechatronics (AIM)*, 2018, pp. 170–175. DOI: 10.1109/AIM.2018.8452263.

[2] M. Xiao, Q. Wen, L. Ji, and W. Wang, "Tennis ball picking robot based on bluetooth control," in *Proceedings of the 2021 2nd International Conference on Control, Robotics and Intelligent System*, ser. CCRIS '21, Qingdao, China: Association for Computing Machinery, 2021, pp. 12–16, ISBN: 9781450390453. DOI: 10.1145/3483845.3483848. [Online]. Available: https://doi.org/10.1145/3483845.3483848.

[3] Zhang, Zhiwei, *Tennis ball collecting device*, https://patents.google.com/patent/CN214232656U/en, CN214232656U. Available at: https://patents.google.com/patent/CN214232656U/en, 2021.

[4] Yanko Design. "The ball boy." Accessed: 2025-05-18. (2014), [Online]. Available: https://www.yankodesign.com/2014/07/30/the-ball-boy/.

[5] H.-C. Kang, H.-N. Han, H.-C. Bae, M.-G. Kim, J.-Y. Son, and Y.-K. Kim, "Hsv colorspace-based automated object localization for robot grasping without prior knowledge," *Applied Sciences*, vol. 11, no. 16, p. 7593, 2021. DOI: 10.3390/app11167593. [Online]. Available: https://doi.org/10.3390/app11167593.

Appendix A Requirement and Verification Table

Table 5: R&V Table For Microcontroller

Requirement	Verification Method
Supports SPI full duplex communication with a speed of $\geq$ 10Mbps	A. Connect the microcontroller to the communication object and logic analyzer through SPI interface; B. Configure SPI clock frequency to 10MHz (main mode) and send 1MB data blocks; C. The receiving end sends back data and records the transmission time; D. Verify the consistency between received and sent data, with a total time of $\leq$ 800ms (rate $\geq$ 10Mbps).
PWM output precision $\leq 0.5\%$	A. Set the PWM frequency to 20kHz, with a duty cycle of 50 %, and connect it to an oscilloscope; B. Measure the PWM pulse width and calculate the deviation between the actual duty cycle and the theoretical value; C. Repeat testing with 10% and 90% duty cycles, and verify that the error is $\leq 0.5\%$.

Table 6: R&V Table For Motor Driver

Requirement	Verification Method
Can drive two DC motors, each supporting a maximum current output of 2A	A. Connect the microcontroller to the communication object and logic analyzer through SPI interface; B. Configure SPI clock frequency to 10MHz (main mode) and send 1MB data blocks; C. The receiving end sends back data and records the transmission time; D. Verify the consistency between received and sent data, with a total time of $\leq$ 800ms (rate $\geq$ 10Mbps).
Supports PWM control for speed regulation, with a frequency range of 1kHz to 50kHz	A. Connect the motor drive board to the DC power supply (VM=12V); B. Connect two motors to the CN1 and CN2 interfaces; C. Use a signal source to provide PWM and EN signals respectively; D. Connect the ammeter and measure the current value of the motor load during operation, ensuring that each output current is not greater than 2A.

Table 7: R&V Table For Battery

Requirement	Verification Method
The battery pack outputs a stable 12V voltage and supports a continuous discharge current of 2A	A. Use electronic loads to test the battery output voltage under different output currents (0.5A/1A/2A); B. Verify that the voltage is maintained at around 12V.

(continued on next page)

(continued from previous page)

Requirement	Verification Method
Supports long battery life and meets the requirement of 4-hour continuous operation	A. Connect the system (motor logic circuit) representing the actual load in a fully charged state; B. Run continuously for 5 hours, record voltage changes and remaining capacity; C. Verify whether it can support continuous operation for 4 hours under typical application loads.
Strong adaptability to dynamic loads	A. Simultaneously connect high loads (such as motors) and low-power modules (such as MCUs, cameras); B. Start the motor and observe whether there is interference or power failure in the logic power supply (3.3V/5V); C. Observe voltage stability through an oscilloscope.

Table 8: R&V Table For DC-DC Voltage Reduction

Requirement	Verification Method
Stable conversion of 12V input to 5V and 3.3V outputs	A. After powering on, measure whether the voltage of VOUT5 and VOUT3.3 is within the range of 5V ± 5% and 3.3V ± 5% respectively; B. Use an oscilloscope to observe the output voltage waveform and confirm that there is no serious overshoot or voltage drop phenomenon.

(continued on next page)

(continued from previous page)

Requirement	Verification Method
The output voltage remains stable during dynamic load changes	A. Simultaneously connect the high-power motor (12V) and the logic module (3.3V/5V); B. Start the motor and monitor the logic voltage output; C. Collect the voltage waveform during operation with an oscilloscope to verify the DC-DC response capability and stability.

Table 9: R&V Table for Ball Collection Mechanism

Requirement	Verification Method
Wall/Corner Collection	
The mechanism shall collect balls located within 2 cm of a wall	A. Mark a test court with 2 cm grid lines adjacent to the wall; B. Place balls at 2 cm distance and activate the mechanism; C. Observe and record whether the ball is successfully collected.
The 90° corner retrieval success rate shall be ≥95%	A. Perform 20 trials of ball placement in 90° corners; B. Record retrieval outcomes using a high-speed camera; C. Calculate success rate and confirm it meets the requirement.
Brush Mechanism	

(continued on next page)

(continued from previous page)

Requirement	Verification Method
Brush rotational speed shall be 60 RPM $\pm$ 5	A. Activate the brush mechanism; B. Use a DT-2236 laser tachometer to measure RPM; C. Repeat measurements and confirm values fall within the specified range.
Brush contact force shall be 2 N $\pm$ 0.2 N	A. Use SH-50 force gauge to measure the contact force between brush and surface; B. Conduct measurements at multiple positions; C. Ensure all measured values lie within the tolerance range.